



Spintronic Materials: Nanostructures and Devices (SMND-2011)

# Surfactant-aided variation in CdO nanocomposites morphology

T. Prakash<sup>a</sup>, T. Arunkumar<sup>b</sup>, D. Sathya Raj<sup>a</sup>, R. Jayaprakash<sup>a\*</sup><sup>a</sup> Nanotechnology Laboratory, Department of Physics, S.R.M.V. CAS, Coimbatore – 641020, Tamil Nadu, India.<sup>b</sup> Solar Laboratory, Department of Physics, S.R.M.V. CAS, Coimbatore – 641020, Tamil Nadu, India.

## Abstract

This paper presents the synthesis of CdO nanocomposites in chemical precipitation method. This article reports the formation of different morphologies of CdO nanocomposites with Polyethylene glycol (PEG) surfactant. This technique emphasizes the less consumption of time for synthesizing nano powder with smaller particle size. This route for preparing CdO is simple and cost-effective method. CdO nanocomposites were characterized by X-ray powder diffraction (XRD), Fourier transform-infrared spectroscopy (FT-IR), TEM measurements, Scanning electron microscope (SEM), Energy dispersive spectrum (EDS) and Electrical resistance. The particle size extracted from XRD patterns, were around 30 nm. The particle size obtained from TEM image is will consistent with XRD pattern. Analytical potential of these nanocomposites has been used to determine the trace levels of polycyclic aromatic compounds in river waters.

© 2013 The Authors. Published by Elsevier B.V. Open access under [CC BY-NC-ND license](https://creativecommons.org/licenses/by-nc-nd/4.0/).

Selection and peer-review under responsibility of the Department of Physics, School of Science and Humanities, Kongu Engineering College

*Keywords:* CdO; semiconductors; nanocomposites; XRD

## 1. Introduction

The cadmium oxide nanocomposites consisting of organic polymers, inorganic polymers and inorganic nanoparticles in a nanoscale regime represent a novel class of materials that have motivated considerable interest in recent years. These composites exhibit new advantageous properties and can be very different from those of their individual counterparts. It is therefore expected that this type of materials will play increasingly important roles in research and in numerous applications. They frequently have special properties and are significant for many technological applications, ranging from microelectronics to catalysis, optoelectronics devices, synthesis of lubricant and preparation of electrolytes for rechargeable batteries [1-4]. Among these materials, semiconductor nanocomposites have recently aroused much attention [5]. II-VI group semiconductor nanomaterials such as CdS, PbS, ZnS and CdSe have been studied extensively due to their strongly size-dependent optical properties. It is well known that nanocrystalline semiconductor exhibits quantum confinement effect and possesses properties that are different from the bulk [6]. Control over both nanocrystalline morphology and particle size by different synthesis routes enables the researchers to obtain the desired properties for the application. There are only very little literature available on the synthesis of the particles as free-standing powder.

\* Corresponding author. Tel.: +91 0422 2692349  
E-mail address: [jprakash\\_jpr@rediffmail.com](mailto:jprakash_jpr@rediffmail.com) .

This work aims at carrying a different morphology obtained by PEG as surfactant. It also helps to get the gel formation, and to obtain the more amount of final product with good crystallinity [7].

## 2. Experimental procedure

### 2.1 Materials

Cadmium chloride ( $\text{CdCl}_2$ ), PEG and ammonia were procured from (Merk, 98%) Mumbai, India. All the chemicals were of analytical grade and used as received without further purification.

### 2.2 Synthesis

The synthesis of CdO nanocomposites were prepared by chemical precipitation method carried out as follows. First, a 0.1 M of cadmium hydroxyl solutions was prepared by dissolving cadmium (II) chloride ( $\text{CdCl}_2$ ) in deionized water. The 1g of PEG mixed with 25 ml of deionized water and is stirred thoroughly. The gel PEG solution added drop wise in 0.1 M cadmium hydroxyl solution. Then pH of the solution was maintained at 8 by adding liquid ammonia drop wise. The precipitate was filtered and washed with double distilled water and ethanol until the solution becomes free from chlorine ions (in the silver nitrate test). Finally the precipitate was transferred into round bottom flask and heated upto  $80^\circ\text{C}$  with constant vigorous stirring and then refluxed for 6 hours. The cadmium oxide powder was obtained. Finally the sample which was considered as as-prepared sample Sample-A and Sample-B. Then the Samples A and B were at  $150^\circ\text{C}$  and  $300^\circ\text{C}$ , respectively, for 5h in ambient atmosphere.

#### 2.2.1 Characterization

The sample microstructure was analyzed by X-ray diffraction (XRD) using a Bruker AXS D8 Advance instrument and the monochromatic  $\text{CuK}_{\alpha 1}$  wavelength of  $1.5406 \text{ \AA}$ . The average crystalline size of the crystallites was evaluated using the Scherrer's formula,

$$d = \frac{K\lambda}{\beta \cos \theta}$$

where  $d$  is the mean crystalline size,  $K$  is a grain shape dependent constant (0.9),  $\lambda$  is the wavelength of the incident beam,  $\theta$  is a Bragg reflection angle and  $\beta$  is the full width at half maximum (FWHM) of the main diffraction peak. The Fourier transform infrared spectra (FT-IR) of the samples were recorded by using a 5DX FTIR spectrometer. The sample morphology was observed by scanning electron microscopy (SEM) with energy dispersive X-ray analysis (EDS) using a JEOL 5600LV microscope at an accelerating voltage of 10 kV. The transmission electron microscopy (TEM) and selected-area electron diffraction (SAED) was recorded on a Technai G20-stwin using an accelerating voltage of 200 kV. The electrical conductivity measurements were carried out using a digital LCR Meter Systronics Mod. 925.

## 3. Results and discussion

### 3.1 Morphological and microstructural analysis

#### 3.1.1 X-Ray diffraction

XRD patterns of sample-A and Sample-B are shown in Fig. 1. The diffraction pattern of Sample-A (Fig. 1a) confirms the higher order of cadmium hydroxyl group  $\text{Cd}(\text{OH})_2$  and small amount of CdO [8]. The sample heated at  $300^\circ\text{C}$  (Sample-B) (Fig. 1b) transfers the  $\text{Cd}(\text{OH})_2$  into good crystalline pure CdO. The samples prepared at this temperature possess higher order of semiconductor property.

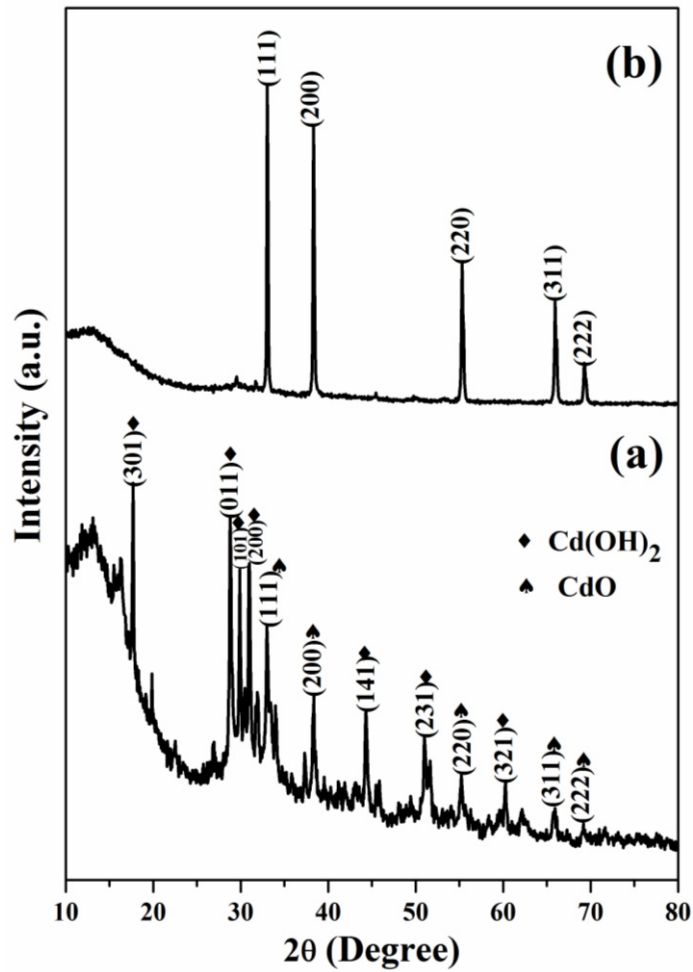


Fig. 1 XRD pattern of cadmium oxide nanocomposites (a) Sample-A; (b) Sample-B

The samples still have a well-defined crystalline structure in the presence of surfactant. XRD pattern of Sample-B exhibited the formation of cubic  $\text{CdO}$  phase crystal structure and indexed the following miller indices (111), (200), (220), (311), (222). The observed diffraction planes were well matched with the (JCPDS 05-0640). This confirms that the refluxing process has converted the cadmium hydroxyl group with PEG into cadmium oxide group and well crystalline  $\text{CdO}$  nanocomposites. The average crystallite size of Sample-B was calculated and found to be 30 nm. The lattice constant of Sample-B were calculated as  $a=4.697\text{\AA}$ , it matches well with standard values [9].

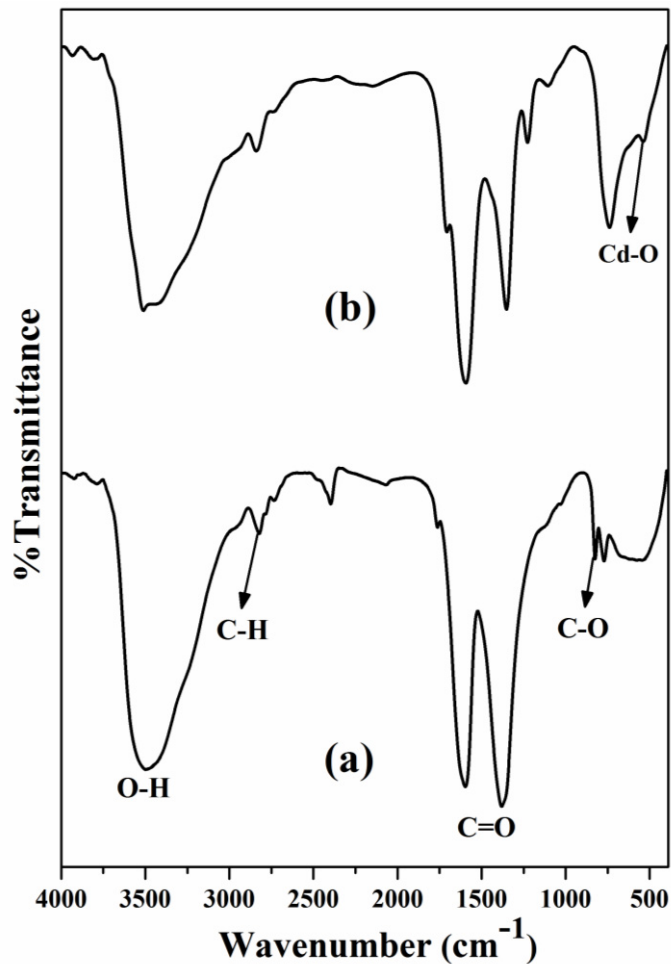


Fig. 2 FT-IR spectrum of cadmium oxide nanocomposites (a) Sample-A; (b) Sample-B

### 3.1.2 Fourier transform infrared spectroscopy

The formation CdO functional group from the cadmium hydroxyl group was also confirmed from FT-IR analysis. The FT-IR spectrum of CdO nanocomposites for Sample-A and Sample-B are shown in Fig. 2. Samples (A&B) show the presence of as-prepared CdO and annealed CdO nanocomposites. Fig. 2(a) shows that absorption peaks of O-H from the hydrogen bonds in the wave number range  $3200 - 3550\text{cm}^{-1}$  [10,11], C-O-C in between  $1085$  to  $1150\text{cm}^{-1}$  [10-12], C-H from alkyl groups between  $2828$  to  $3000\text{cm}^{-1}$ , C=O from  $1737$  to  $1750\text{cm}^{-1}$  [13], and C-O (crystallinity) at about  $1141\text{cm}^{-1}$  [14]. In Fig. 2(b), a peak observed around  $420\text{cm}^{-1}$  is assigned to Cd-O of CdO which confirms the formation of pure CdO nanocomposites. The other peak at  $3400\text{cm}^{-1}$  corresponds to the absorbed water vapour after bringing the specimen out of the furnace [15].

### 3.1.3 Surface morphology

The morphology of the synthesized nanocomposites were analysed by scanning electron microscope (SEM). A typical micrograph of Sample-A and Sample-B is shown in Fig. 3. Fig. 3 (a, a1) is apparent from the micrograph that the overall morphology is agglomeration of particles. Fig. 3 (b, b1) is

reveal that the non agglomeration of particles due to the increase of temperature. The surface morphology of cadmium oxide nanocomposites showed the presence of particles composed by the agglomeration and non agglomeration of smaller crystallites [16].

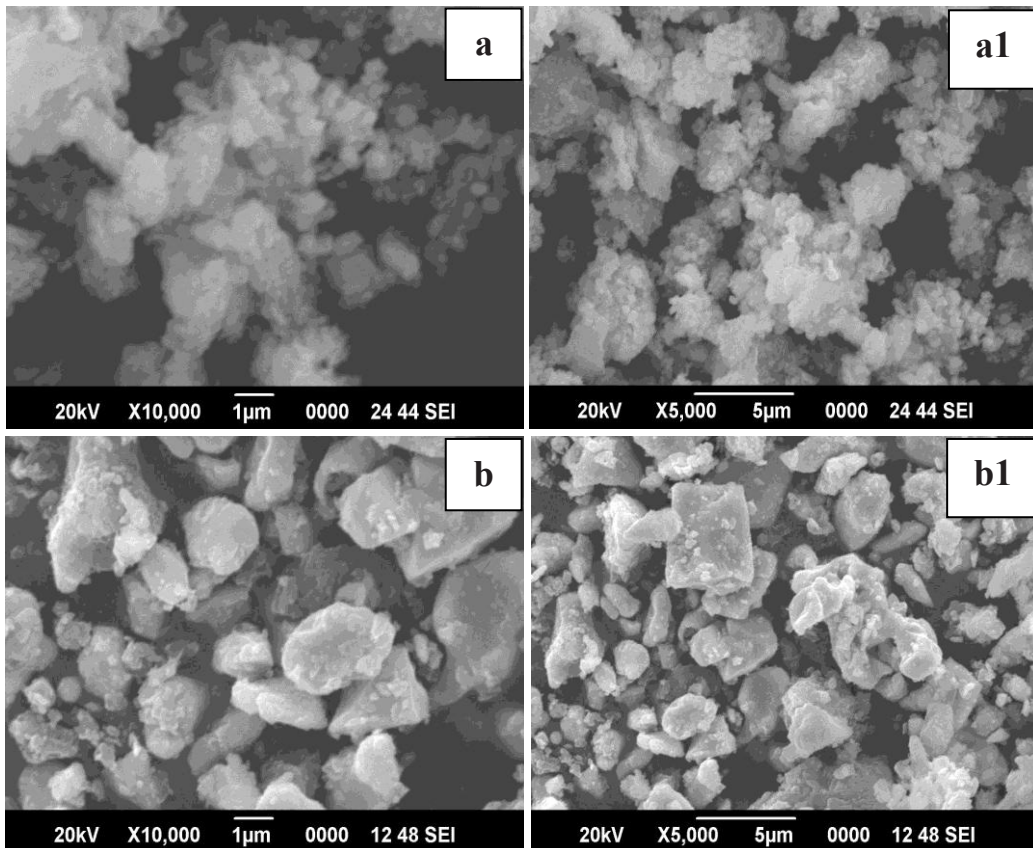


Fig. 3 SEM micrograph of CdO nanocomposites (a) Sample-A; (b) Sample-B

### 3.1.4 EDS spectrum

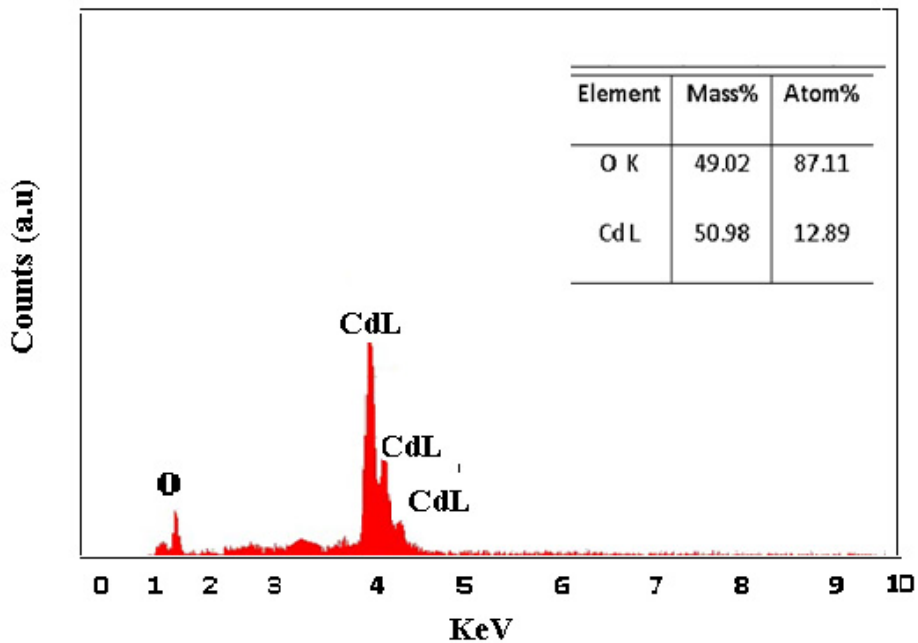


Fig. 4 EDS spectrum of cadmium oxide nanocomposites for Sample- B

The EDS spectrum is given in Fig. 4 which shows the presence of cadmium oxide as the only compound [17].

### 3.1.5 TEM observation

The TEM micrograph and SAED pattern of CdO nanocomposites Sample-B is shown in Fig. 5. The transmission electron microscopy (TEM) of the powder dispersed in organics showed that the particles are agglomerated a small amount of spherical particle present due to the PEG. However, the picture indicates that the spherical shapes particle of the diameter in nanometer regime. The observed particle size was in the range of 33-40 nm. These values are in very good agreement with the particle size calculated from XRD measurements. The corresponding SAED pattern inset of Fig. 5 showed the bright spots which confirmed the presence of the crystalline phase of the cubic CdO structure.

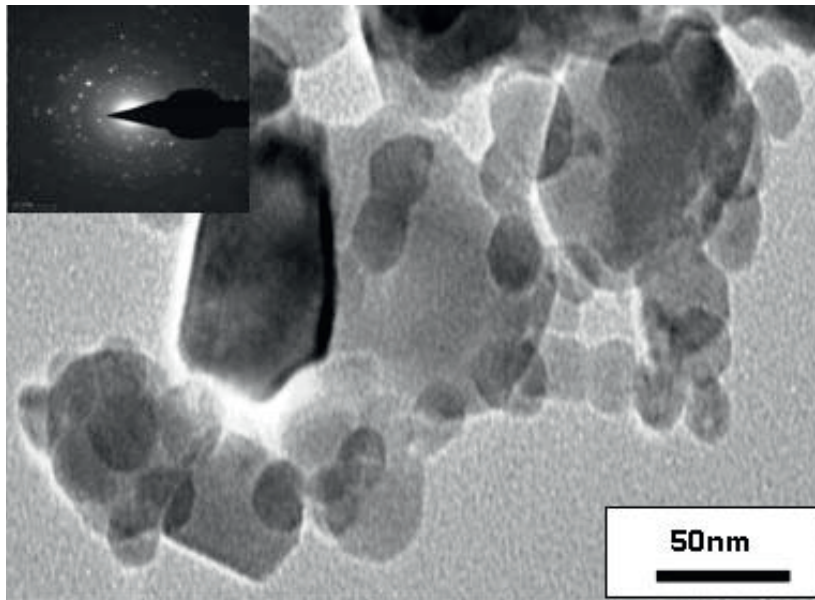


Fig. 5 TEM micrograph of cadmium oxide nanocomposites for Sample-B

### 3.2 Electrical resistivity measurement

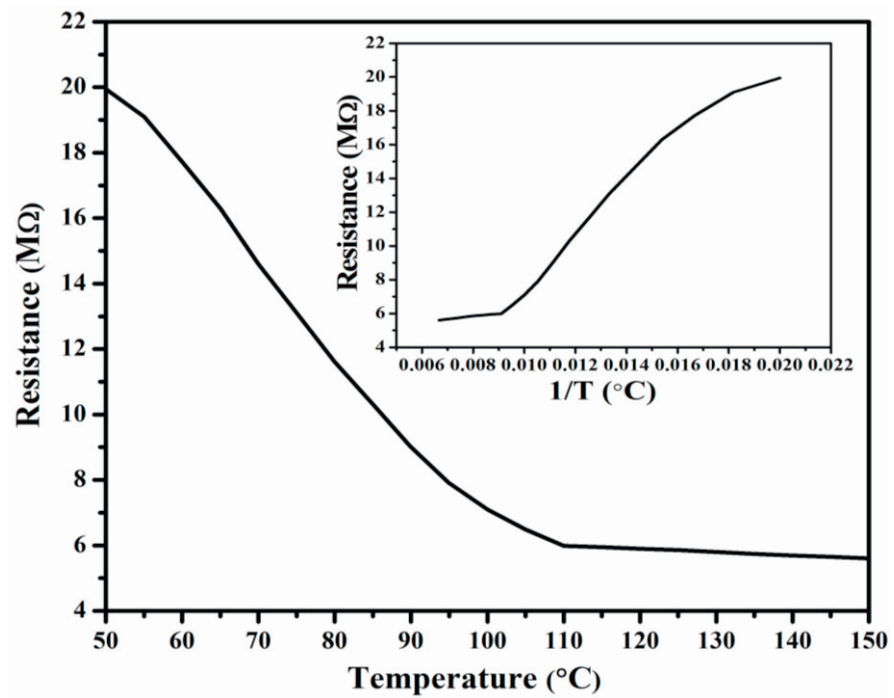


Fig. 6 Variation of electrical resistance of cadmium oxide nanocomposites for Sample-B



Fig. 6 shows the variation of dc resistivity with temperature of Sample- B. At room temperature, the electrical resistance was found to be around 20 M $\Omega$ . The plot resistance vs. temperature shows two regions of resistance. Initially, the resistance decreases strongly with the temperature increase suggesting a semiconductor behavior. The resistance decrease in the temperature range from 110 to 150°C is instead much more limited. This suggests that more than one conduction mechanisms is involved. In the first region, at temperatures between RT and 110°C, conduction is due to the increase in electron concentration and mobility with rise in temperature while, above 110°C and up to 150°C, the conduction mechanism is likely due to polaron hopping [18]. Then, we have plotted resistance versus 1/T, which is shown as inset of Fig. 6.

#### 4. Conclusion

The CdO with surfactant PEG nanocomposites were prepared in chemical precipitation method. This work aims at carrying a different morphology obtained by using the surfactant. It modifies the shapes of the particle into spherical, it analysed different temperatures of SEM analysis. The average particle size of the CdO nanocomposites predicted from XRD result is consistent with the observed particle size from TEM micrograph (33-40nm). The concentration of the CdO nanocomposites was low as a very weak vibration peak of Cd-O bonding at 420 cm<sup>-1</sup> is observed in the FT-IR spectrum. The resistivity of CdO nanocomposites is found to be very low 20 M $\Omega$  at 50°C while it is 5 M $\Omega$  at 150°C.

#### References

- [1] Hirakawa, S., Yamada, K., Bae, J.M., *Solid Ionics*. 118 (1999) 29.
- [2] Trindade, T., Neves, M.C., Barros, A.M.V., *Scr. Mater.* 43 (2000) 567.
- [3] Chen, S., Liu, W.M., Yu, L.G., *Wear*. 218 (1998) 153.
- [4] Krawiec, W., Scanlon, Jr.J.G., Vasudevan, S., *J. Power Sources*. 54 (1995) 310.
- [5] Vijayakumar, R., Palchik, O., Gednake, A., *Ultrason. Sonochem.* 9 (2002) 65.
- [6] Nanda, K.K., Sarangi, S.N., Mohanthy, S., *Thin Solid Films*. 322 (1998) 21.
- [7] Guha, P., Ganguli, D., Chaudhuri, S., *Mater. Letters*. 58 (2004) 2963.
- [8] Singh, N., Charan, S., Patil, K.R., *Mater. Letters*. 60 (2006) 3492.
- [9] Lu, H.B., Liao, L., Li, H., Tian, Y., *Mater. Letters*. 62 (2008) 3928.
- [10] Saha, B., Das, S., Chapttopadhyay, K.K., *Sol. Energy Mater. Sol. Cell*. 91 (2007) 1692.
- [11] Coates, J., *Encyclopedia of analytical chemistry*, John Wiley&sons, Chichester; 2000.
- [12] Andrade, G., Barbosa-Stancioli, E.F., Mansur, A.A.P., Vasconcelos, W.L., Mansur, H.S., *J. Mater. Sci.* 43 (2008) 450.
- [13] Mansur, H.S., Sadahira, C.M., Souza, A.N., Mansur, A.A.P., *Mater. Sci. Eng. C*. 28 (2008) 539.
- [14] Mallapragada, S.K., Peppas, N.A., *J. Polym. Sci. B: Polym. Phys.* 34 (1996) 1339.
- [15] Bazargan, A.M., Fateminia, S.M.A., Esmailpour Ganji, M., Bahrevar, M.A., *Chem. Eng. J.* 155 (2009) 523.
- [16] Campbell, K., Duncan, Q.M., *Int. J. Pharma.* 363 (2008) 126.
- [17] Bazaragan, A.M., Fateminia, S.M.A., Esmailpour Ganji, M., Bahrevar, M.A., *Chem. Eng. J.* 5 (2009) 523.
- [18] Sawant, V.S., Shinde, S.S., Deokate, R.J., Bhosale, C.H., Chougule, B.K., Rajpure, K.Y., *Appl. Surf. Sci.* 255 (2009) 6675.